Investigation of the Charge Distribution in Titanium Carbide Using Electromigration*†

D. L. Kohlstedt‡
Department of Physics and Materials Research Laboratory, University of Illinois, Urbana, Illinois 61801
and
Wendell S. Williams
Department of Physics, Department of Ceramic Engineering, and Materials Research Laboratory, University of Illinois, Urbana, Illinois 61801
(Received 20 April 1970)

The diffusion of carbon in single crystals of the compound TiC_x ($x \sim 0.9$) near 2000 °C is shown to be influenced by the application of an electric field. This effect, electromigration, was studied using the electron probe microanalyzer to determine the carbon concentration profile. The effective charge Z^* of the diffusing carbon particle was found to be positive. However, Z^* includes both an electrostatic charge Z and a term resulting from momentum exchange with the current carriers. It is argued that the momentum exchange term is small because the carrier concentration is low compared to most metals, and negative because the carriers are predominantly electrons rather than holes. Hence, the observation that Z^* is positive indicates that Z is also positive. C thus diffuses as a positive ion in TiC, though at a lattice site it may appear negative, as has been suggested by recent energy-band calculations and by electron spectroscopy and x-ray experiments, because of the overlap of Ti wave functions. An average value for the energy of motion of C (vacancies) in TiC_x of 4.8 ± 0.5 eV/atom was also obtained. This value is consistent with the results of Sarian on tracer diffusion of C^{14} in TiC_x crystals.

I. INTRODUCTION

The cubic transition-metal carbides are complex solids combining ionic structure, metalic conductivity, and covalent strength.[1-5] The nature of these isomorphs of the alkali halides is further complicated by the ability of the carbon sublattice to accommodate up to 50% vacancies. Despite the intricate combination of physical properties exhibited by the carbides, recent research has provided a substantial foundation on which to build an understanding of their character. Investigations of transport properties have found a high metallic resistivity that suggests the existence of a low density of electronic charge carriers, as well as demonstrating the importance of electron and phonon scattering by C vacancies.[6,7] Studies of the great strength of the carbides indicate that this property is intrinsic and results from exceptionally strong atomic bonding.[2,8,9] The unusually high melting temperatures which are characteristic of the carbides are also a result of this strong bonding.[1] For a deeper understanding of the properties of the carbides, a more detailed interpretation of the bonding must be given.

Energy-band calculations can yield predictions of the spatial distribution and angular momenta of electrons in a solid and, consequently, can lead the way to an interpretation of bonding. Several energy-band calculations for TiC have been published recently.[10-14] Although all the calculations give similar spatial distributions of electronic charge about the atomic sites, the calculations differ as to the "true" charge of the C and Ti ions, that is, as to the number of electrons transferred between crystal states derived from C p states and Ti s and d states. Even the direction of electron transfer is disputed. A calculation by Lye[13] using linear combinations of atomic orbitals (LCAO) gives electron transfer from C to Ti, whereas augmented-plane-wave (APW) calculations by Ern and Switendick[11] and by Conklin and Silversmith[10] have electron transfer from Ti to C. Consequently, two quite different models for bonding in TiC exist. New experimental evidence is needed to test predictions of the conflicting energy-band calculations and to guide the development of an adequate model for bonding in these solids.

Optical reflectivity studies, which provide information relevant to the band structure, have already been performed.[12] These results, in fact, provide the basis for one of the existing band calculations.[13] The other band structures do not agree well with the optical-reflectivity results, but there is controversy over the reasons for and significance of such lack of agreement. Fermi-surface studies could be related to the energy-band calculations, but such measurements are not possible in TiC because the high density of vacancies produces an unusually short scattering time and prevents the development of oscillatory effects.

Recent electron spectroscopy and x-ray studies have examined the charge distribution around the C and Ti atoms at their equilibrium positions.[15,16] The results confirm the predictions of all the energy-band calculations that excess electronic charge exists around the C atom, but they do not convincingly distinguish between the band calculations on points of disagreement, in particular, the nucleus with which this charge is associated (i. e., the true charge of C and Ti).

An experiment that could distinguish between the

two types of atoms by sampling their charge distributions separately was sought. Reststrahlen studies are ruled out by the presence of free carriers. However, the very defects which prevent the establishment of oscillatory behavior, carbon vacancies, can be exploited to distinguish between C and Ti atoms in a study of diffusion.

For diffusion by a vacancy mechanism, the activation energy is the sum of the energy of formation and the energy of motion of a vacancy. In TiC_x, the fraction of "chemical" vacancies, $1-x$, far exceeds the thermal equilibrium fraction. Consequently, only motional energy is involved in the self-diffusion of C. For Ti self-diffusion in TiC_x, both energies are involved. Hence, diffusion of C in TiC is orders of magnitude more rapid than that of Ti.[17]

Diffusion biased by an electric field, electromigration, offers the possibility of studying only the charge associated with the C ion. The results of such an investigation are reported here.

II. ELECTRON ENERGY-BAND STRUCTURE OF TiC

A. APW Energy-Band Calculations

In their APW calculations for TiC, Ern and Switendick[11] use the crystalline potentials obtained from a self-consistent solution to the Hartree-Fock-Slater equations starting with neutral atomic configurations for Ti and C. Qualitatively, Ern and Switendick's calculation shows that electrons are transferred from Ti $3d$ states to the C $2p$ states. This model predicts strong metal-metal and metal-nonmetal interactions with only a small ionic contribution to the total cohesive energy.

Conklin and Silversmith[10] have calculated energy bands for TiC using the muffin-tin APW crystal potentials from a superposition of atomic charge densities, a superposition of $Ti(4s^0)^{++}$ and $C(2p^4)^{--}$ ionic charge densities, and a self-consistent charge density starting from the doubly ionized configuration. Only small differences exist in the results of these three calculations. The results support the general character of Ern and Switendick's band structure. Conklin and Silversmith conclude that bonding in TiC is predominantly covalent. They find that, although between two and three electrons are transferred from Ti orbitals to C orbitals, the spatial charge transfer from Ti to C is less than one electron due to the diffuse nature of the wave functions involved. Thus, the ionic bonding between Ti and C arises from less than one electronic charge. However, for optical studies which depend upon the amount of charge that moves with each type of nucleus, they suggest that an ionic charge of between one and three electronic units may be involved since the C nucleus will carry the charge which is localized near it and has the symmetry of C states.

B. LCAO Energy-Band Calculations

In contrast to the APW calculations, which stress theoretical self-consistency, an LCAO calculation by Lye[13] is based on, and is hence internally consistent with, optical-reflectivity data obtained by Logothetis.[12] The LCAO wave functions are also adjusted so that the band structure accounts qualitatively for Hall coefficient, thermopower, magnetic susceptibility, resistivity, piezoresistivity, and photoemission data.[13]

In Lye's model, the Ti $3d$ states are lower in energy than the C $2p$ states and thus receive electronic charge from the C atoms. The Ti $3d$ wave functions then overlap onto the C sites making the potential at the C site more negative and, consequently, raising the C $2p$ energy levels. The final result is that 1.25 electrons are transferred from C $2p$ states to states derived from the Ti $3d$ states. However, the *spatial* charge transfer is from the Wigner-Seitz cell around the Ti site to the Wigner-Seitz cell around the C site due to the enlarged radial distribution of the Ti wave functions.[18]

The predominant contribution to bonding according to Lye's model results from covalent metal-metal bonds similar to those in the transition metals. However, the bonds are strengthened by the presence of C atom core potentials in the region of overlap of the Ti $3d$ orbitals, as proposed in an earlier LCAO calculation by Costa and Conte.[14] The presence of an increased number of Ti $3d$ electrons, coming from C $2p$ orbitals, also strengthens the metal-metal bonding. Covalent Ti-C and C-C bonds also contribute to the bonding of TiC. Ionic bonding contributes little to the cohesive energy.

Thus, the results of the energy-band calculation of Lye differ from those of Ern and Switendick[11] and of Conklin and Silversmith,[10] with respect to the direction of charge transfer and, hence, the nature of the bonding. The present experiment was designed partly to distinguish between the two possibilities by determining the charge on a moving (diffusing) C atom.

III. ELECTROMIGRATION

A. Theories

Electromigration is biased diffusion resulting from an applied, static electric field.[19–21] The most obvious effect of the electric field on the diffusing ions is the electrostatic force. In addition, a "friction" or "electron-wind" force arises from momentum transfer between conduction electrons (holes) and diffusing ions. It drives the ions against (with) the electrostatic force. For a specific resistivity for defects ρ_d/N_d, a specific resistivity for the bulk ρ/N, and an applied electric field E,

Huntington and Grone[22] have shown that the force F on a diffusing atom can be expressed by

$$F = eE\left[Z - \gamma_e\left(\frac{\rho_{ed}}{N_d}\right)\left(\frac{N}{\rho_e}\right)\left(\frac{m_e^*}{|m_e^*|}\right) - \gamma_h\left(\frac{\rho_{hd}}{N_d}\right)\left(\frac{N}{\rho_h}\right)\left(\frac{m_h^*}{|m_h^*|}\right)\right] , \quad (1)$$

where e is the magnitude of the electronic charge, Z is the electrostatic charge of the diffusing ion, γ is the electron-atom ratio, and m^* is the effective mass of the charge carriers. The subscripts e and h signify electrons and holes, respectively. The electron- and hole-scattering terms are summed over all bands. The direction of the electron or hole contribution to the frictional force depends on the sign of the current carriers through the effective mass.

Fiks[23] has also presented an expression for the force on an ion during electromigration,

$$F = eE(Z - n_e\Lambda_e\Sigma_e + n_h\Lambda_h\Sigma_h) , \quad (2)$$

where Λ is the mean free path, Σ is the atomic cross section for ions scattering electrons, and n is the density of current carriers. Bosvieux and Friedel[24] have preformed a quantum-mechanical calculation which yields a form similar to those of Eqs. (1) and (2) for the driving force.

The equations for the net electromigration force can be written in the form

$$F = eEZ^* , \quad (3)$$

where Z^* is the electromigration effective charge and includes both the electrostatic and frictional effects. The driving force acting on a diffusing ion is related to its average drift velocity v caused by this force through the Nernst-Einstein relation

$$v = (D/fkT)F , \quad (4)$$

where k is Boltzmann's constant, T is the temperature, D is the diffusion coefficient, and f is the correlation factor. Thus, for electromigration,

$$v = (D/fkT)eEZ^* . \quad (5)$$

The direction of the wind depends on the signs and mobilities of the current carriers.

B. Studies of Electromigration

For most pure metals with electrons as the charge carriers, the electron-wind force is larger than the electrostatic force. Mass is therefore transported toward the anode with a drift velocity corresponding to an effective charge of magnitude greater than 1. For example, $Z^* = -3$ for Cu,[25] $Z^* = -25$ for Ag,[26] $Z^* = -9$ for Au,[27] and $Z^* = -20$ for Al.[27] For metals with large positive Hall coefficients (hole conductors), mass flow during electromigration is toward the cathode. For γ-Fe, $+1 \leq Z^* \leq 3$[28] and for Co, $Z^* = 1.6$.[29] Thus, the hole wind dominates the electrostatic force.

Electromigration studies of interstitial C in γ-Fe, interstitial C in Ti, and C in Co-bonded WC are of particular relevance to the present work. In γ-Fe containing C and in TiC the metal atoms are arranged on a fcc lattice with C occupying octahedral intersitital sites. However, there is a large difference in C concentration between the two systems. For C in γ-Fe, Dayal and Darken[30] found $Z^* = +3.7$. From measurements of Z^* as a function of temperature, Kovenskii[31] calculated an electrostatic charge Z of $+3.8$ for C in the same system. For the entire temperature range considered (850–1200 °C), Z^* was positive ($+10.8$ – $+8.7$) and decreased with increasing temperature. A study of electromigration in dilute C in bcc Ti has also been reported.[31,32] From measurements of Z^* as a function of temperature, an electrostatic charge of $+4.0$ was determined. Values of Z^* were not reported. Hehenkamp and Heumann[33] observed electromigration of C toward the cathode in Co-bonded WC.

C. Attempts to Separate Electrostatic and Frictional Effects

Two principal methods have been proposed for separating the effect of the electrostatic force from the electron-ion scattering force. An analytical method has been developed by Smolin and Frantsevich.[34] Their development uses Fiks's formalism of Eq. (2). For a one-band solid and for Σ and n independent of temperature, they find that

$$Z^* = \frac{H}{T + \rho_0/\beta} + Z , \quad (6)$$

where the bulk resistivity is $\rho = \rho_0 + \beta T$ and H is a constant. Therefore, Z^* as a function of temperature can be used to determine Z. This technique has been used to give $Z = +0.76$ in Ni.[35] Studies on dilute C-interstitial migration in several transition metals have yielded $Z = +4.0$ in Ti, $Z = +2.8$ in Ta, and $Z = +0.6$ in W.[32,36]

An experimental separation of the electrostatic force from the frictional force was suggested by Miller,[37] who proposed studying electromigration in a Hall field. The Hall field is perpendicular to the direction of flow of the charge carriers as well as to the direction of the applied electric and magnetic fields. The transport of ions parallel to the Hall field is controlled by the Hall-field force and thus provides a measure of the electrostatic charge only. Using this method, Miller[37] concluded that at 825 °C Fe diffuses in Ge as trivalent, positively charged ions. Bibby and Youdelis[38] reported values for Z of $+4.3$ and $+5.7$ for C and N, respectively. These values are within experimental error of Pauling's[39] metallic valences of $+4e$ for C and $+5e$

for N.

Two difficulties accompany the Hall-field technique. First, except for ferromagnetic materials, the Hall field in most metals is too small to produce a measurable transport of mass. Second, as Huntington[40] has noted, the influence of the momentum transfer to ions by charge carriers cannot be eliminated in complex metals because in the Hall experiment both holes and electrons move toward one side of the specimen.

IV. EXPERIMENTAL METHOD

A. Electron Microprobe

In the present work, the primary method used for determining the concentration profile of C in TiC resulting from electromigration was electron-microprobe analysis. The electron microprobe chemically analyzes samples by bombarding them with energetic electrons and measuring the resulting characteristic x-ray intensities for each element present. The x-ray intensity of a given characteristic line can be related to the weight percent of the corresponding element which is present in the sample.[41,42]

Although the electron microprobe has been used frequently to measure the concentration profiles for diffusion couples,[43] only recently has it been employed in studies of electromigration.[44] Compared to the radioactive-tracer[45] and the surface-marker motion[22] techniques for studying electromigration, the electron-microprobe approach has both advantages and disadvantages. The electron-microprobe technique provides a relatively fast determination of concentration profiles from which the electromigration force is determined, but it is limited to alloys. It is nondestructive and can be used for systems where no radioactive tracer is available. The electron-microprobe approach also avoids the difficulties inherent with surface phenomena, such as surface diffusion, condensation, and evaporation, which complicate the study of surface-marker motion.

B. Theoretical Concentration Profiles

Fick's second law

$$\frac{\partial C}{\partial t} = -\frac{\partial J}{\partial y} = \frac{\partial}{\partial y}\left(D\frac{\partial C}{\partial y}\right) \tag{7}$$

describes the temporal t and spatial y changes in concentration C during diffusion, where J is the atomic current. If the atoms experience an external force during their diffusion jumps, then Fick's second law must be modified[46] to account for the additional atomic current $J = vC$. Thus Eq. (7) becomes

$$\frac{\partial C}{\partial t} = \frac{\partial}{\partial y}\left(D\frac{\partial C}{\partial y} - vC\right) \quad . \tag{8}$$

When D and v are independent of concentration and the diffusion zone is isothermally heated, Eq. (8) simplifies to

$$\frac{\partial C}{\partial t} = D\frac{\partial^2 C}{\partial y^2} - v\frac{\partial C}{\partial y} \quad . \tag{9}$$

Closed-form solutions for the concentration as a function of time and position can be found for this equation given the initial and boundary conditions.

In the experiment, single crystals of TiC were mounted between C electrodes and then Joule-heated to diffusion temperatures. A constant source of C was therefore available at both ends of the TiC sample, because Ti diffusion outward is much slower than C diffusion inward.[17] The boundary condition for the above geometry is $C(0, t) = C(L, t) = C_{max}$. The initial condition is that the TiC crystal has a homogeneous C concentration, $C(y, 0) = C_0$. The concentration profile at time t and position y for a crystal of length L is given by[47]

$$C(y, t) = C_{max} - (C_{max} - C_0)(2\pi)e^{vy/2D}\sum_{m=1}^{\infty}\frac{m\sin(m\pi y/L)}{(vL/2D)^2 + (m\pi)^2} \times \exp\left\{-\left[\left(\frac{vL}{2D}\right)^2 + (m\pi)^2\right]\frac{Dt}{L^2}\right\}\left[1 - (-1)^m e^{-vL/2D}\right] \quad . \tag{10}$$

This concentration profile is shown in Fig. 1 for several values of the diffusion parameter $\Delta = Dt/L^2$ and the asymmetry parameter $V = vL/2D$. To find these electromigration parameters, the theoretical prediction for the concentration profiles is fitted to the experimental data.

As shown above, the analysis of experimental data for *constant* diffusion coefficient and constant drift velocity can be handled by solving the boundary-value problem arising from a modified form of Fick's second law. However, the electron microprobe cannot be used in electromigration studies with vanishingly small concentration gradients and hence constant D and v. In the present work, the diffusion coefficient and drift velocity are assumed to be constant and are found by the curve-fitting procedure described above. The justification for these approximations and the actual concentration dependence of the diffusion coefficient are considered in Sec. V.

C. Electromigration Anneals

Single crystals of TiC were used in this work. They were grown at the Linde Division of Union Carbide Corporation by the arc-Verneuil process. Mass spectrographic analysis showed less than 100 at. ppm impurities and chemical analysis revealed less than 0.02 wt. % O and N.[8]

Initial electromigration experiments were performed on long, thin crystals (approximately 1 mm $\times$1 mm$\times$10 mm) in $\frac{3}{4}$ atm of high-purity A. The

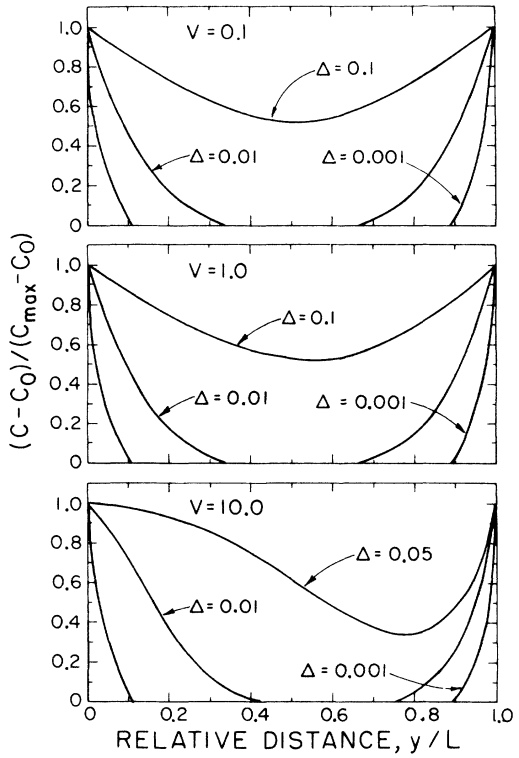

FIG. 1. Theoretical curves of concentration versus penetration distance as described by Eq. (10) in the text.

A atmosphere was used to reduce the effects of vaporization at the elevated temperatures (near 2000 °C) used. The initially homogeneous crystals, generally $TiC_{0.94}$, were supported between and in direct contact with spectroscopic graphite electrodes. Electron-microprobe analysis showed that Ti did not diffuse from the crystal into the C electrodes. Thus, the boundary condition for this geometry is that both ends of the crystal are in contact with infinite sources of C as described above and hence always at the limiting composition, $TiC_{0.97}$. Diffusion times were chosen to give a gradient in C concentration extending in from each end approximately one-third the length of the crystal. However, near the center of each crystal in the region not affected by C diffusion into the crystal from the electrodes, the C- to-Ti ratio was found to have changed from its initial value. The final C-to-metal ratio near the center was smaller than its initial value, suggesting that substantial vaporization had occurred and that C vaporization was more rapid than Ti vaporization. The latter result is contrary to the findings for vaporization from TiC in a vacuum[6] and probably indicates that the A gas scatters Ti atoms back toward the sample more efficiently than it scatters C atoms. Oxygen impurity would also reduce x.

To reduce the net flux of atoms from the surface, several electromigration runs were performed in a stainless-steel system which was pressurized to 25 atm of A. However, noncongruent vaporization still influenced the bulk C-to-Ti ratio. Therefore, cylindrical samples of $TiC_{0.84}$ with small length-to-diameter ratios were used for the remainder of the experiments so that the surfaces not in contact with the electrodes could be approximated as being infinitely far from the central axis of the crystal. These final experiments were also performed in 25 atm of A. In this situation only diffusion of C from the electrodes into the crystal influenced the C-to-Ti ratio along the central axis.

An optical pyrometer was used to measure the temperature. For the 2.5-mm-long by 4-mm-diam sample, no measurable temperature gradient was observed along the length of the sample. For the longer samples (7.5 mm by 4 mm), readings taken near each end and near the center generally agreed to within less than 10 °C. Some uncertainty arises in measuring the surface temperature, since the local surface condition influences the measurement. Emissivity corrections were made from temperature readings in a 20-mil-deep 15-mil-diam spark-eroded hole in a TiC crystal. Window corrections were also made.

D. Determination of Concentration Profiles

A well-annealed single crystal of $TiC_{0.94}$, as determined by chemical analysis, was used as a standard for obtaining the C and Ti concentrations from the electron-microprobe intensities. The raw x-ray intensities were converted to weight percent Ti and weight percent C by a computer program written by Colby[48] and modified by Gray[42] which corrects for deadtime losses, background as a function of composition, absorption, characteristic line fluorescence, atomic-number effects, and beam-current fluctuations. In addition to the sample data, the Ti and C concentrations of each standard datum point were calculated relative to the average of the standard readings to provide reference data. The reference data taken before and after the sample traverse were compared. Differences between the two sets of reference data reflected drift in the microprobe electronics. If the drift exceeded 0.2 wt.% in the C concentration, the sample data were rejected. A detailed discussion of the electron-microprobe analysis is presented elsewhere.[49]

The analysis of light elements, including C, using the electron microprobe is difficult. In addition to the problem of converting the raw data to weight percents, there exists the more fundamental problem of detecting the low-energy C x rays, due to substantial absorption of and low peak-to-background ratio for the C x rays.

For comparison, the concentration profile of one

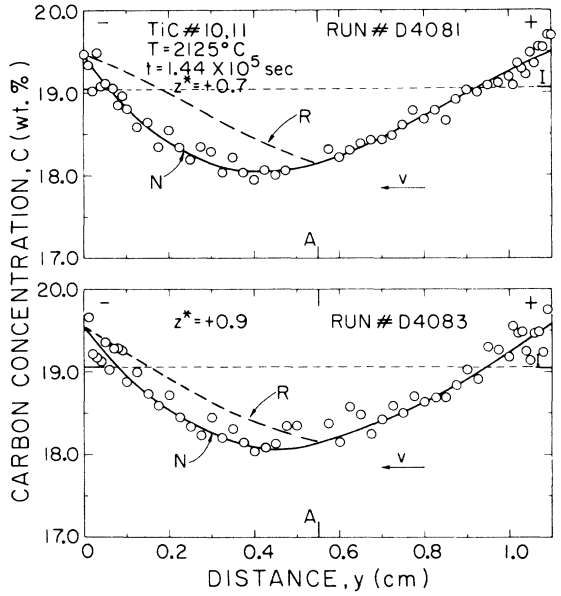

FIG. 2. C concentration versus penetration distance for electromigration in TiC #10, 11. The solid line N is the curve determined by a least-squares fit of the data to Eq. (10) and the broken line R is a reflection of the right half of N. A marks the center of the profile, I the initial concentration, v the direction of the electromigration velocity, and + and − the polarity of the applied voltage.

crystal was also determined by microhardness studies. The microhardness of TiC has been established as a function of C concentration.[15,50] A Knoop diamond indenter with 25-g load was used to make the microhardness indentations. Twenty-two rows of eleven indentations each were made along the length of the crystal. The indentations were approximately 20 μ long and were aligned along a $\langle 100 \rangle$ crystal axis with the indentation length perpendicular to the length of the crystal and on a $\{100\}$ cleavage plane. The microhardness H_μ determined from the length of each indentation was converted to a C-to-metal ratio using the relation

$$x = 0.075 + (3.1 \times 10^{-5}) H_\mu \ , \qquad (11)$$

where H_μ is in kg/mm^2. This equation was determined from a least-squares fit of the experimental data of Williams[50] and Ramquist.[15]

V. EXPERIMENTAL RESULTS

Electron-microprobe analyses of several control samples showed that the crystals were initially homogeneous in C distribution to within the accuracy of the analyses, ± 0.2 wt. %. For the long, thin crystals heated in $\frac{3}{4}$ atm of A, the diffusion penetration depths are approximately an order of magnitude larger than the half-widths of the samples. Two electron-microprobe analyses of one of these four crystals are shown in Fig. 2 with the initial concentration denoted by I.

Diffusion constants were determined from the vaporization-dependent concentration profiles of these four crystals by curve fitting the profiles to Eq. (10), which does not account for vaporization. The resulting diffusion constants correspond to diffusion temperatures 200 to 600 °C higher than the actual experimental temperatures. However, the effective charge determined for a sample with a concentration profile that is influenced by vaporization (TiC #10, 11) is in good agreement with the effective charge determined from a sample, to be discussed below, which was studied at the same temperature but with a concentration profile not influenced by vaporization (TiC #12, 6, 3). Therefore, the effect of vaporization on the asymmetry is evidently small.

The concentration profile determined by microhardness measurements on TiC #10, 1 is shown in Fig. 3. The effective charge of + 0.5 determined from this profile is in reasonable agreement with the effective charges of + 0.4 and + 0.7 determined from concentration profiles obtained by electron-microprobe analyses. However, the concentration profile determined by the microhardness technique (Fig. 3) differs by a scale factor from the concentration profiles found by the electron-microprobe analyses. The agreement can be substantially improved by using only Williams's[50] microhardness versus C-to-metal ratio data which are for single-

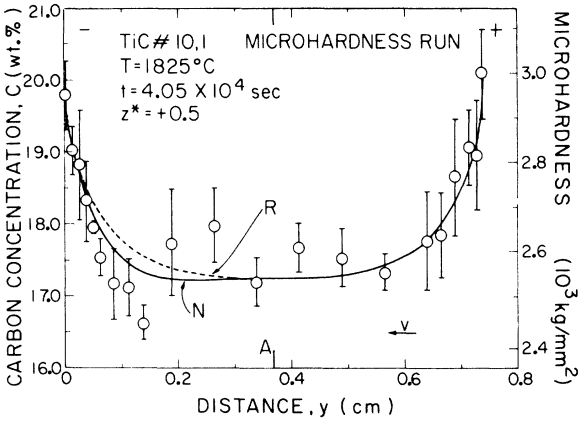

FIG. 3. C concentration as determined from microhardness measurements versus penetration distance for TiC #10, 1. The solid line N is the curve determined by a least-squares fit of the data to Eq. (10) and the broken line R is a reflection of the right half of N. A marks the center of the profile, v the direction of the electromigration velocity , and + and − the polarity of the applied voltage.

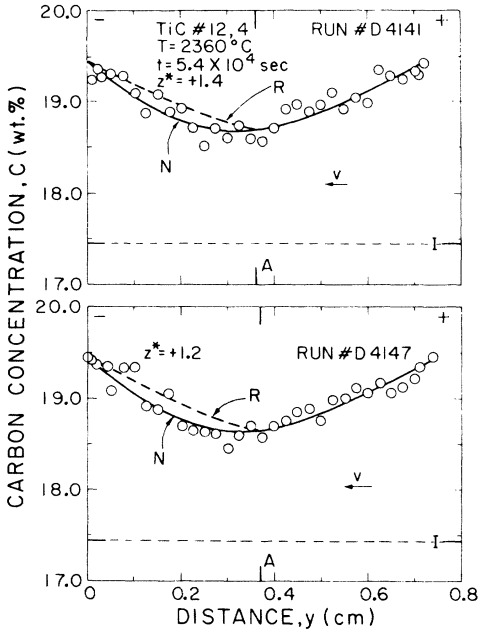

FIG. 4. C concentration versus penetration distance for electromigration in TiC #12, 4. The solid line N is the curve determined by a least-squares fit of the data of Eq. (10) and the broken line R is a reflection of the right half of N. A marks the center of the profile, I the initial concentration, v the direction of the electromigration velocity, and + and − the polarity of the applied voltage.

crystal samples and neglecting Ramquist's[15] results which include data from polycrystalline samples.

The concentration profiles of another group of five crystals with larger cross-sectional areas did not reflect the influence of vaporization. Two typical electron-microprobe analyses of one of these five crystals are shown in Fig. 4. To check the effect of vaporization, the samples were also probed perpendicular to the central electromigration axis. The concentration was found to be homogeneous for at least 0.5 mm on either side of the central axis. Further evidence for the lack of influence of vaporization is seen in the concentration profiles of TiC #12, 2; TiC #12, 6, 3; and TiC #12, 5. These profiles have minima near 17.45 wt.% which is the initial C concentration of the crystals. The minima for samples TiC #12, 3 and TiC #12, 4 are at higher C concentrations because these samples were heated for times long enough to permit C to diffuse from the ends to the middle. Finally, the activation energy of 4.8 ± 0.5 eV/atom calculated from the concentration profiles of these five samples (Fig. 5) is in reasonable agreement with that determined from diffusion experiments performed on similar samples, 4.2 ± 0.3 eV/atom.[49] Hence, the approximation D = const and v = const used in the analysis appears to be justified.

The data from several electron-microprobe analyses for each sample were curve fitted by the method of least squares to the equation appropriate for electromigration with the given initial and boundary conditions, Eq. (10). Approximately ten electron-microprobe analyses were made on each crystal. Those analyses that showed large drift (0.2 wt.% C) were rejected. The curve N determined by the least-squares fit is drawn with the data points (Figs. 2 and 4). The right half of the least-squares curve is also reflected R onto the left-hand side to help depict the asymmetry. The initial C concentration I, the center of the crystal A, the direction of the electromigration velocity v, and the polarity + or − of the applied voltage are also marked.

The experimental parameters measured explicitly and those determined from curve fitting the data from two electron-microprobe analyses for each crystal to Eq. (10) are presented in Tables I and II. The values for the electromigration effective charge calculated from these parameters, the diffusivities calculated from the measured temperatures using our recently reported chemical diffusivities,[49] and the diffusivities that were found from

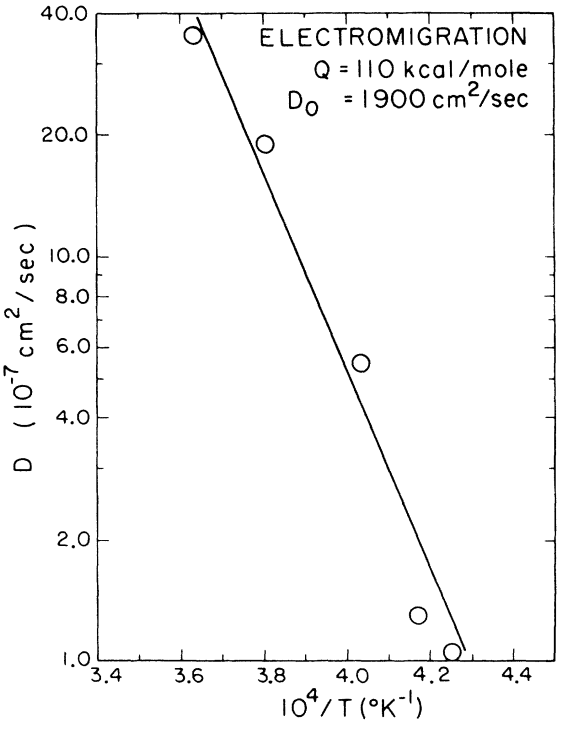

FIG. 5. Chemical diffusivity versus reciprocal temperature. These data, whose calculations are described in the text, are for electromigration crystals TiC #12, 2; TiC #12, 6, 3; TiC #12, 3; TiC #12, 4; and TiC #12, 5.

TABLE I. Experimental parameters from the electromigration experiments on TiC.

Sample	Run	$V=vL/2D$	$\Delta = Dt/L^2$	L (cm)	t (sec)	j (A/cm^2)
10, 1	D4045	−0.46	0.08	0.76	4.05×10^4	1.8×10^3
	D4046	−0.85	0.06			
10, 3	D4050	−0.22	0.10	0.56	7.56×10^4	2.2×10^3
	D4051	−0.30	0.10			
10, 2	D4043	−1.74	0.09	0.72	7.20×10^4	2.0×10^3
	D4044	−1.82	0.11			
10, 11	D4081	−1.44	0.08	1.09	1.44×10^5	2.5×10^3
	D4083	−0.92	0.10			
12, 2	D4093	−0.46	0.016	0.70	8.77×10^4	7.5×10^2
12, 6, 3	D4253	−0.08	0.012	0.24	5.28×10^3	8.8×10^2
	D4256	−0.16	0.012			
12, 3	D4122	−0.74	0.073	0.81	8.67×10^4	8.4×10^2
	D4155	−0.39	0.070			
12, 4	D4141	−0.68	0.123	0.73	5.4×10^4	8.8×10^2
	D4147	−0.57	0.119			
12, 5	D4173	−1.55	0.028	0.73	3.6×10^3	9.9×10^2
	D4175	−3.10	0.021			

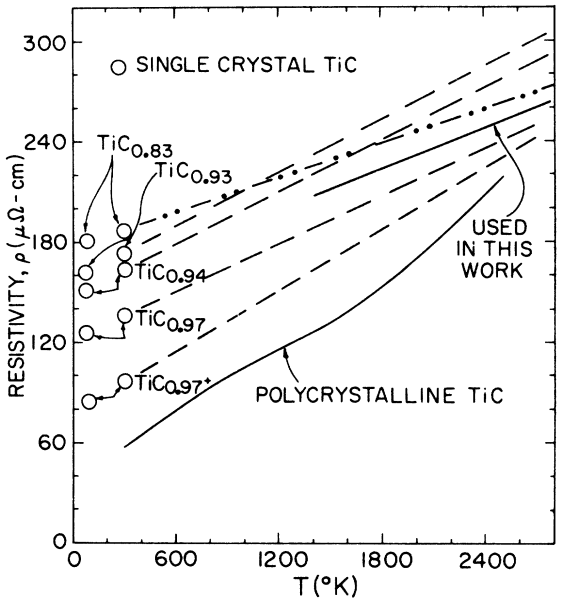

FIG. 6. Electrical resistivity versus temperature for TiC. The single-crystal data are from Williams (Ref. 6) and were extrapolated to diffusion temperatures; the polycrystalline data are from a compilation by Touloukian (see Ref. 54).

the least-squares analyses are also tabulated. The effective charge was determined from Eq. (5), where the correlation factor was taken as that appropriate for diffusion by a vacancy mechanism on a fcc lattice $f=0.78$, v/D was found from the asymmetry parameter of the curve fit, and the electric field was found from the measured current density and literature values of the resistivity shown in Fig. 6. It should be noted that the correlation factor is a function of concentration in carbide-like systems which have large densities of vacancies on one sublattice; f as a function of concentration can take on values between 0.78 (fcc lattice with only thermal vacancies) and 1.00 (interstitial diffusion on a fcc lattice) for a monovacancy mechanism in such systems. However, it is consistent with the assumption that D and v are independent of concentration to use a constant value for f. The parameters found from the curve fit are the diffusion parameter $\Delta = Dt/L^2$ and the asymmetry parameter $V = vL/2D$.

TABLE II. Experimental parameters from the electromigration experiments on TiC. $D=[L^2\Delta/t]$ is the chemical diffusivity determined from curve fitting the experimental concentration profiles to Eq. (10), and $D[T]$ is the chemical diffusivity determined from the measured temperature.

Sample	Run	ρ (μΩ cm)	T(°C)	$D=[L^2\Delta/t]$ (cm^2/sec)	$D[T]$ (cm^2/sec)	Z^*	$\bar{Z}^*$
10, 1	D4045	235	1825	15×10^{-7}	0.14×10^{-7}	+0.4	$+0.5_5$
	D4046			11		0.7	
10, 3	D4050	238	1875	4.1	0.21	0.2	0.2_5
	D4051			4.1		0.3	
10, 2	D4043	244	2025	6.5	0.84	1.6	1.6_5
	D4044			7.9		1.7	
10, 11	D4081	248	2125	6.5	1.7	0.7	0.8_0
	D4083			8.2		0.9	
12, 2	D4093	246	2080	0.9	1.5	1.1	1.1_0
12, 6, 3	D4253	248	2125	1.4	2.2	0.5	0.7_5
	D4256			1.3		1.0	
12, 3	D4122	251	2210	5.5	4.4	1.4	1.0_5
	D4155			5.3		0.7	
12, 4	D4141	257	2360	12.1	6.3	1.4	1.3_0
	D4147			11.7		1.2	
12, 5	D4173	262	2480	40.8	30.0	2.9	2.8_0
	D4175			30.5		2.7	

To check the value of the effective charge determined from Eq. (10), the effective charge was also calculated by a second approach for TiC #12, 6, 3. The average penetration depths from the positive and negative electrodes were taken to be

$$\langle y\rangle_{\pm} = \langle y\rangle_{\text{diff}} \pm \langle y\rangle_{\text{elec}} , \tag{12}$$

respectively, where $\langle y\rangle_{\text{diff}}$ is the average penetration depth due to diffusion and $\langle y\rangle_{\text{elec}}$ is the average penetration depth due to electromigration. The average penetration depths were calculated from the equation

$$\langle y\rangle = \frac{\int_{y_0}^{y_{\max}} (C - C_0) y\, dy}{\int_{y_0}^{y_{\max}} (C - C_0)\, dy} , \tag{13}$$

where y_0 and $y_{\max}$ correspond to C_0 and $C_{\max}$, respectively, and $y_0 = L/2$. The drift velocity can be written in terms of the electromigration penetration depth as

$$v = (\langle y\rangle_+ - \langle y\rangle_-)/(2t) \tag{14a}$$

$$= \langle y\rangle_{\text{elec}}/t . \tag{14b}$$

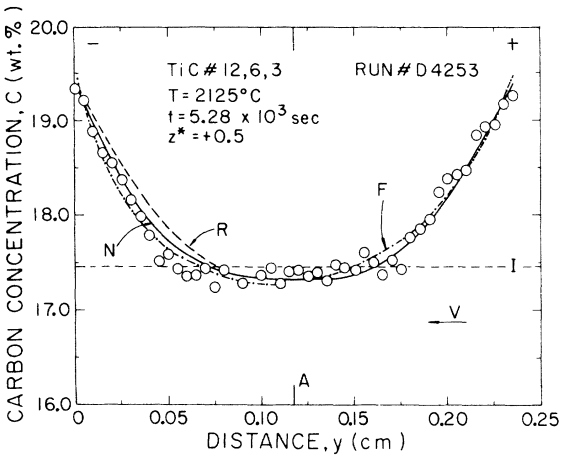

FIG. 7. C concentration versus penetration distance for electromigration in TiC #12, 6, 3. The solid line N is the curve determined by a least-squares fit of the data to Eq. (10), the broken line R is a reflection of the right half of N, and the broken line F was determined by a least-squares fit of the data to Eq. (15). A marks the center of the profile, I the initial concentration, v the direction of the electromigration velocity, and + and − the polarity of the applied voltage.

The concentration as a function of position for this approach was calculated from a least-squares fit to the arbitrary equation

$$C(y) = A^0 + \exp(A_0 + A_1 w + A_2 w^2 + A_3 w^3) , \qquad (15)$$

where the A's are constants. This form was chosen because it followed the data well. The resulting curve F for run #4253 of TiC #12, 6, 3 is shown in Fig. 7 with the curve N calculated using Eq. (10). The effective charge of + 1.1 for run #4256 (Table II) found by this method is in good agreement with the value of + 1.0 determined from the curve fit to Eq. (10). Less satisfactory agreement was obtained from run #4253 (Table II), + 1.0 compared to + 0.5. This later result reflects the fact that the function given in Eq. (15) is more sensitive to scatter in the data than is the function given in Eq. (10).

The effective charge versus temperature has been plotted for the nine electromigration crystals in Fig. 8. The values of effective charge are averages of two electron-microprobe analyses per sample. The error bars represent estimated errors due to temperature gradients and the standard deviation for the analyses.

In general, the uncertainty in this work in measuring effective charges by studying the asymmetry in concentration profiles is approximately 50%. The method involves measuring small differences in rather large concentration gradients; therefore, scatter or drift in the experimental data can cause substantial error. A comparison of the values for the effective charge determined by two separate electron-microprobe analyses for the same sample reflects the latter difficulty (Table II). However, there is no doubt about the principal qualitative result: The effective charge of the diffusing C ion is positive in the vicinity of 2000 °C.

VI. DISCUSSION

The electromigration phenomenon has been discussed as a combination of two forces, an electrostatic force and an electron-ion scattering force. It was suggested earlier in this work that a determination of the charge on C ions in TiC might be possible through a study of electromigration. The determination of even the sign of this charge would be valuable in testing the conflicting predictions of the energy-band calculations concerning the direction of electron transfer between C and Ti.

Huntington and Grone's[22] expression for the effective charge, Eq. (1), as modified to include both electron and hole scattering, can be used to analyze the possibility of separating the electrostatic and scattering contributions to the effective charge in a manner similar to that of Smolin and Frantsevich,[34] which was discussed above. Equation (1) is more useful here if it is rewritten in terms of mobilities

$$Z^* = [Z - (1/\mu_{ed} N_d)(n_e \mu_e) + (1/\mu_{hd} N_d)(n_h \mu_h)] \qquad (16a)$$

$$= [Z - (1/\mu_{ed} N_d)(1/e\rho_e) + (1/\mu_{hd} N_d)(1/e\rho_h)] . \qquad (16b)$$

The present experiment shows that for C in TiC the electromigration effective charge Z^* is positive.

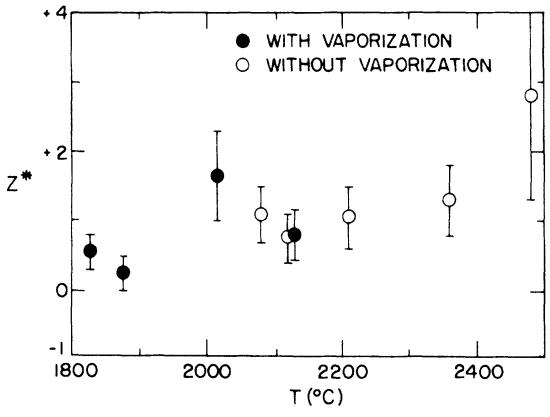

FIG. 8. Electromigration effective charge versus temperature for TiC. The solid circles are data determined from concentration profiles which were influenced by vaporization (TiC #10) while the open circles are data determined from concentration profiles not influenced by vaporization (TiC #12).

In addition, it may be temperature dependent. The value of the effective charge appears to increase from approximately +0.4 at 1825 °C to possibly as high as +2.8 near 2480 °C. Below 1700 °C no electromigration was observed.[51] The zero effect found in our earlier work could reflect the fact that the experimental times were too short to produce a measurable effect or that substantial vaporization occurred during the longer anneals thus masking any electromigration asymmetry. It can be seen from Fig. 8 that if Z^* is temperature dependent, an extrapolation of Z^* to lower temperatures could possibly lead to a negative effective charge. However, because of the large uncertainty in the highest-temperature point, a constant value of $Z^* = 1.0$ also would be consistent with the data. We believe that the latter interpretation, $Z^* \simeq$ constant, is the more plausible.

There are two important parts of the argument that Z^* is constant. First, an increase of the effective charge with temperature would be unusual behavior for a metallic conductor, such as TiC. In most pure metals, the (negative) effective charge *decreases* in magnitude with increasing temperature because the bulk mobility decreases[22,27] [see Eq. (16a)]. Second, room-temperature Hall coefficient measurements suggest that the conduction in TiC is predominately by electrons rather than by holes. These measurements give a value of approximately 0.04 conduction electron/atom,[6,7] a very small value compared to 1 conduction electron/atom for simple metals. Hence, in TiC we anticipate that the electron-ion scattering force should be small compared to the electrostatic force and that it should be antiparallel to the electrostatic force. If this position is correct, then our observation of a positive effective charge ($Z^* > 0$) implies that the electrostatic charge is positive ($Z > 0$). For $Z^* \simeq +1$ independent of temperature, $Z^* \simeq Z \simeq +1$.

Because the electric field affects the diffusing ion during its entire jump, we suggest that the measured value of the electrostatic charge Z is the average value

$$Z = (a_{\max} - a_0)^{-1} \int_{a_0}^{a_{\max}} Z(a)\, da \quad , \tag{17}$$

where a_0 is the position of the initial equilibrium site, $a_{\max}$ is the position locating the top of the migration barrier, and $Z(a)$ is the charge which is affected by the electric field when the ion is at position a of the diffusion jump. The electrostatic charge, which is the charge sensed by the electric field, should be distinguished from the effective charge Z^* which is the charge measured in the electromigration experiment. The effective charge includes contributions from the electrostatic charge and the momentum transfer between diffusing ions and charge carriers. The true charge Z_{true} discussed earlier is the charge associated with the C nucleus, thus excluding charge resulting from overlap of Ti orbitals onto the C ion.

The energy-band calculations all predict that $Z(a_0)$ is negative for C in TiC. However, as the C ion makes a diffusion jump, the overlap of the Ti orbitals onto the moving ion will change in some complex manner from the configuration at the equilibrium lattice site. Thus, the C ion may appear negative to the electric field at its equilibrium site but positive in regions along the jump path if $Z_{\text{true}} > 0$. A hypothetical variation with position of the electrostatic charge associated with the diffusing C ion is shown in Fig. 9 with $Z(a_{\max}) > 0$ and $Z(a_0) < 0$. Clearly, Z as defined by Eq. (17) can be positive even if $Z(a_0)$ is negative provided that Z_{true} is positive. The true charge is illustrated in Fig. 9 as being larger than $Z(a)$ for all jump positions, a situation which occurs if the diffusing ion is always shielded to some degree by Ti $3d$ overlap. A value of $Z \simeq +1$ is consistent, in terms of the above model, with the band-structure prediction of $Z_{\text{true}} = +1.25$ by Lye.[12,13]

Although a temperature-dependent effective charge is less plausible, this result could be analyzed with Eq. (16). The *electrostatic* charge is assumed to be independent of temperature. Therefore, an increase in the effective charge with increasing temperature could be due to one of three effects. First, if the conduction in TiC is by electrons alone as has been suggested from the low-temperature Hall data,[6,7] then the temperature dependence of the effective charge which may be present could reflect the fact that the hole-scattering force is zero and

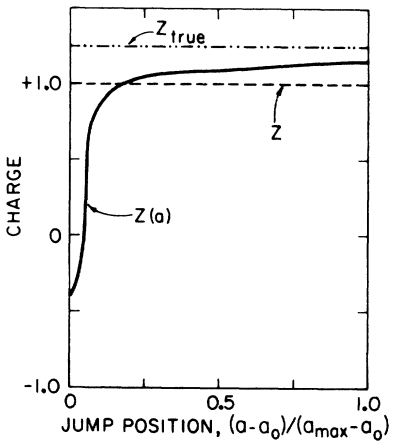

FIG. 9. Three charge values associated with C particle in TiC: Z is the average value suggested by present experiment; $Z(a)$ is the instantaneous value (hypothetical) during diffusion jump; Z_{true} is the value obtained from energy-band calculation for charge identified with only C nucleus (see Ref. 13). Because of overlap of Ti $3d$ wave functions, $Z(a)$ is negative at C lattice site and $Z < Z_{\text{true}}$.

the electron-scattering force becomes smaller as the resistivity becomes larger. That is, the negative term in Eq. (16) becomes smaller as the temperature increases so that Z^* approaches $Z>0$. Second, if the hole-scattering term is important, then an increase in the effective charge with increasing temperature could reflect an increase in the hole-scattering term relative to the electron-scattering term. This second situation would arise if the hole resistivity increased less rapidly than the electron resistivity with increasing temperature [see Eq. (16b)]. Such a variation in hole and electron resistivities could arise from different rates of change with temperature of their mobilities or from changes in the densities of charge carriers with temperature [see Eq. (16a)]. Third, a complex arrangement could be imagined in which several bands participate with different temperature dependences both for their mobilities and for their densities of carriers.

If the data of Fig. 8 are interpreted to mean that Z^* is temperature dependent, and if the first of the above three explanations is adopted, then an approximate value for the electrostatic charge can be determined from the data for Z^* versus temperature using Eq. (8). The necessary resistivity-versus-temperature information is shown in Fig. 6. A value of $Z=+10$ is obtained with $\beta=4\times10^{-2}$ $\mu\Omega$ cm/°K and $\rho=150$ $\mu\Omega$ cm, which were obtained by extrapolation from lower-temperature resistivity data.[6] If high-temperature data for polycrystalline specimens are used instead, $\rho_0=0$ and β is not needed. Then $Z=+4$, if the two points with extremely high values of Z^* are omitted. Clearly, +10 is too large for the true charge on the C ion, but +4 is a value often found by electromigration for C in metals.[30–32,38]

Although the value $Z=+10$ is probably not the fairest statement of the results of this experiment, such a high positive value would indicate the presence of a substantial contribution to the current-

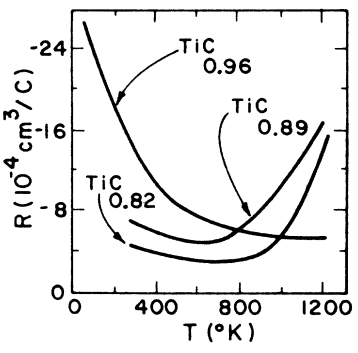

FIG. 10. Hall coefficient versus temperature for TiC with $0.82\leq x\leq0.96$ (Golikova *et al.*, see Ref. 52).

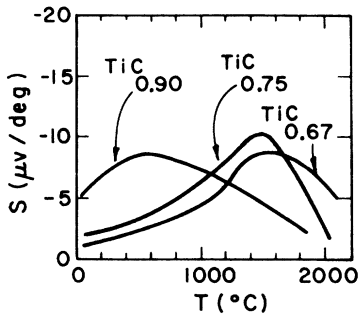

FIG. 11. Thermoelectric power versus temperature for TiC_x with $0.67\leq x\leq0.90$ (Golikova *et al.*, see Ref. 53).

ion interaction from holes. Some evidence for the existence of holes in TiC can be found in the temperature dependences of the Hall coefficient[52] and thermoelectric power[53] at high temperatures. These quantities are plotted versus temperature in Figs. 10 and 11, respectively. Although the Hall coefficient data extend only to 900 °C, it appears that a simple, one-carrier model is not adequate for TiC at high temperatures. The thermoelectric power versus temperature for three C-to-metal ratios is shown in Fig. 11. The thermoelectric power is clearly not simple in TiC. Qualitatively, the minimum and the increase toward zero in the thermoelectric power are consistent with the proposal that the hole resistivity is increasing less rapidly with increasing temperature than is the electron resistivity.

However, there is no evidence that hole conduction becomes dominant in TiC at 2000 °C. Furthermore, the carrier concentration appears to be much lower than in most metals,[6,7] and hence momentum exchange with the diffusing ion should be relatively less important. Therefore, we believe that the principal effect in the electromigration of C in TiC is the direct influence of the electric field on a positive C ion.

Ramqvist[15] has studied the spectroscopy of photo and Auger electrons, x-ray emission, and x-ray absorption in the group IV *B* and group V *B* transition-metal carbides under monochromatic x-ray irradiation. The results indicate that the charge distribution is such that the metal atoms are positive and C atoms are negative at their equilbrium sites $Z(a_0)<0$. An x-ray diffraction study of the charge density in NbC by Merisalo and co-workers[16] supports Ramqvist's results. Ramqvist interprets his experimental data by means of Hartree-Fock and Hartree-Fock-Slater calculations on free atoms and ions to show that metal atoms lose *d* electrons. Since the interpretation of the present work distinquishes between the total electronic charge around the C nucleus and the electronic charge that moves

with that nucleus, the result is not inconsistent with the qualitative result that the C charge at the equilibrium lattice site is negative (see Fig. 9). However, the present result contrasts with Ramqvist's conclusion that *d* electrons are transferred from Ti orbitals to C orbitals.

The proposed model is thus also consistent with the theoretical result which was obtained by all three of the recent energy-band calculations that the C ion appears negative at its equilibrium site. However, it supports the tight-binding calculation[12,13] rather than the APW calculations[10,11] in that it suggests that the average electrostatic charge and also the true charge of C in TiC is positive. The numerical value of electrostatic charge as obtained from this experiment is between +1 and +4.

The implications for bonding are hence those associated with the LCAO calculation, namely, the principal contribution is from a strengthened metal-metal interaction from the participation of nonmetal electrons and a lowering of the potential between metal atoms due to the presence of the C atoms.

ACKNOWLEDGMENTS

The authors are grateful to J. B. Woodhouse who advised and instructed us on the electron-microprobe work, D. Walter who performed the microhardness measurements, and S. Rotz who assisted with the data taking and computer programming. Discussions with K. Bachmann, G. Emmons, A. Gerk, L. Radosevich, and L. Shacklette were very valuable. C. P. Flynn, D. Lazarus, A. B. Liddiard, J. W. McClure, T. Rowland, and C. P. Slichter provided illuminating suggestions on specific theoretical problems.

---

*Work supported in part by the U. S. Atomic Energy Commission under Contract No. AT(11-1)-1198.

†Paper based on a thesis submitted by D. L. Kohlstedt to the Graduate College of the University of Illinois, Urbana, Illinois in partial fulfillment of the requirements for the Ph. D. degree.

‡Present address: Surface Physics, Cavendish Laboratory, University of Cambridge, Cambridge, England.

[1]W. S. Williams, Science 152, 34 (1966).

[2]G. E. Hollox, Mater. Sci. Eng. 3, 121 (1968).

[3]*Fundamentals of Refractory Compound*, edited by H. H. Hausner and M. G. Bowman (Plenum, New York, 1968).

[4]P. Schwartzkopf and R. Kieffer, *Refractory Hard Metals* (MacMillan, New York, 1953).

[5]E. K. Storms, *The Refractory Compounds* (Academic, New York, 1967), Vol. II, p. 3.

[6]W. S. Williams, Phys. Rev. 135, A505 (1964).

[7]J. Piper, J. Appl. Phys. 33, 2394 (1962).

[8]W. S. Williams and R. D. Schaal, J. Appl. Phys. 33, 955 (1962).

[9]W. S. Williams, J. Appl. Phys. 35, 1329 (1964).

[10]J. B. Conklin, Jr., and D. J. Silversmith, Int. J. Quantum. Chem. IIS, 243 (1968).

[11]V. Ern and A. C. Switendick, Phys. Rev. 137, A1927 (1965).

[12]R. G. Lye and E. M. Logothetis, Phys. Rev. 147, 622 (1966).

[13]R. G. Lye, in *Atomic and Electronic Structure of Metals* (American Society for Metals, Metals Park, Ohio, 1967), p. 99.

[14]P. Costa and R. R. Conte, J. Nucl. Met. 10, 19 (1964).

[15]L. Ramqvist, Jernkont. Ann. 153, 1 (1969).

[16]M. Merisalo, O. Inkinen, M. Jarvinen, and K. Kurki-Suonio (private communication)

[17]S. Sarian, J. Appl. Phys. 40, 3515 (1969).

[18]Although the opposite direction of spatial charge transfer was proposed by Lye in Ref. 13, in recent private communication he indicates that his energy-band calculation actually predicts the spatial charge redistribution discussed here.

[19]J. Verhoeven, Met. Rev. 8, 311 (1963).

[20]Y. Adda and J. Philibert, *La Diffusion dans les Solides* (Presses Universitaires de France, Paris, 1966), Vol. II, p. 893.

[21]N. L. Peterson, in *Solid State Physics*, edited by F. Seitz, D. Turnbull, and H. Ehrenreich (Academic, New York, 1968), Vol. XXII, p. 409.

[22]H. B. Huntington and A. R. Grone, J. Phys. Chem. Solids 20, 76 (1961).

[23]V. B. Fiks, Fiz. Tverd. Tela 1, 16 (1959) [Soviet Phys. Solid State 1, 14 (1959)].

[24]C. Bosvieux and J. Friedel, J. Phys. Chem. Solids 23, 123 (1962).

[25]A. R. Grone, J. Phys. Solids 20, 88 (1961).

[26]P. S. Ho and H. B. Huntington, J. Phys. Chem. Solids 27, 1319 (1966).

[27]R. V. Penney, J. Phys. Chem. Solids 25, 335 (1964).

[28]H. Hering and H. Wever, Acta Met. 15, 377 (1967).

[29]P. S. Ho, J. Phys. Chem. Solids 27, 1331 (1966).

[30]P. Dayal and L. S. Darken, Trans. AIME 188, 1156 (1950).

[31]I. I. Kovenskii, Fiz. Tverd. Tela 5, 5 (1963) [Soviet Phys. Solid State 5, 1036 (1963)].

[32]I. N. Frantsevich and I. I. Kovenskii, Dopovidi Akad. Nauk Ukr. RSR 11, 1471 (1961).

[33]T. Hehenkamp and T. Heumann, Arch. Eisenhuettenw. 33, 1 (1962).

[34]M. D. Smolin and I. N. Frantsevich, Fiz. Tverd. Tela 3, 2115 (1961) [Soviet Phys. Solid State 3, 1536 (1962)].

[35]D. F. Kalinovich, I. I. Kovenskii, and M. D. Smolin, Fiz. Tverd. Tela 10, 569 (1968) [Soviet Phys. Solid State 10, 447 (1968)].

[36]I. N. Frantsevich and I. I. Kovenskii, Dopovidi Akad. Nauk Ukr. RSR 9, 1169 (1961).

[37]Yu. G. Miller, Fiz. Tverd. Tela 3, 2382 (1961) [Soviet Phys. Solid State 3, 1728 (1961)].

[38]M. J. Bibby and W. V. Youdelis, Can. J. Phys. 44, 2362 (1966).

[39]L. Pauling, J. Am. Chem. Soc. 69, 542 (1947).

[40]H. B. Huntington (private communication).

[41]K. Keil, Fortschr. Mineral. 44, 4 (1967).

[42]L. J. Gray, Ph. D. thesis, University of Illinois,

1969 (unpublished).
[43]See, for example, J. Philibert, J. Inst. Metals 90, 241 (1962); J. V. P. Long, in *Advances in X-Ray Analysis*, edited by W. M. Mueller and M. Fay (Plenum, New York, 1963), Vol. VI, p. 282; Y. Adda, M. Beycler, A. Kirianenko, and P. Pernot, Mem. Sci. Meto. 57, 423 (1960).
[44]T. Hehenkamp, J. Appl. Phys. 39, 3928 (1968).
[45]H. M. Gilder and D. Lazarus, Phys. Rev. 145, 507 (1966).
[46]J. R. Manning, *Diffusion Kinetics for Atoms in Crystals* (Van Nostrand, Princeton, 1968), p. 170.
[47]B. J. Boltaks, in *Diffusion in Semiconductors*, translated by J. I. Carasso, edited by H. J. Goldsmid (Academic, New York, 1963), p. 93.
[48]J. W. Colby (private communication).
[49]D. L. Kohlstedt, W. S. Williams, and J. B. Woodhouse, J. Appl. Phys. 41, 4476 (1970).
[50]W. S. Williams, in *Propriétés Thermodynamiques Physyes et Structurales des dérivés Semi-Métalliques* (Editions du Centre National de la Recherche Scientifique, Paris, 1967), p. 181.
[51]D. L. Kohlstedt and W. S. Williams, Bull. Am. Phys. Soc. 14, 389 (1969).
[52]O. A. Golikova, F. F. L. Feigel'man, A. I. Avgustinik, and G. M. Klimashin, Fiz. Tekhn. Polup. 1, 293 (1967) [Soviet Phys. Semicond. 1, 236 (1967)].
[53]O. A. Golikova, E. O. Dzhatarov, A. I. Avgustinck, and G. M. Klimashin, Fiz. Tverd. Tela 10, 168 (1968) [Soviet Phys. Solid State 10, 124 (1968)].
[54]*Thermophysical Properties of High Temperature Materials*, edited by Y. S. Touloukian (MacMillan, New York, 1967), Vol. V., p. 178.

PHYSICAL REVIEW B VOLUME 3, NUMBER 2 15 JANUARY 1971

Electron-Phonon Effects in the Infrared Properties of Metals

P. B. Allen
Bell Telephone Laboratories, Murray Hill, New Jersey 07974
(Received 1 September 1970)

Electron-phonon contributions to the infrared absorption in metals are examined from two points of view. First, "golden-rule" calculations are given for normal metals and superconductors which reproduce the phenomenological theory used by Joyce and Richards to analyze their data in lead. This theory is expected to be valid for weak electron-phonon coupling. Second, the Holstein transport theory for normal metals is used to examine the corrections arising from strong coupling. Solutions are found for the response function at general frequencies and wave vectors. The results are similar in form to the golden-rule theory, and provide a simple correction factor to this theory. It is suggested that optical measurements on both normal and superconducting materials may provide a valuable tool for analyzing the coupled electron-phonon system.

In a recent letter, Joyce and Richards[1] (JR) have reported the observation of phonon contributions to the far-infrared absorptivity in lead. The experiments were done at 1.2 °K both for the superconducting and the normal state (by the application of a 1200-G magnetic field). The important feature of the JR experiment is an additional absorption above what is expected for a collisionless electron gas. This extra absorption is ascribed by JR to the Holstein mechanism[2] in which the incident photon is absorbed in a second-order process involving creation of both a phonon and an electron-hole pair. Evidence for this mechanism is the fact that the onset of the extra absorption occurs in the frequency range of abundant phonons, 30–70 cm^{-1}, in normal lead, while in superconducting lead the onset appears to be shifted up by 22 cm^{-1}, which is 2Δ, or the minimum energy required to create an electron-hole pair in the superconducting state.

To further substantiate their identification of the Holstein mechanism, JR presented a semiquantitative theory in which they assume the absorption scales as the density of final states for the combined electron, hole, and phonon with energy conservation the only constraint. This theory seemed to give a fairly satisfactory explanation of the structure that was observed in the ratio of superconducting-to-normal-state absorption. However, the theory had a number of deficiencies. The absolute magnitude of the effect was not predicted. The role of momentum conservation was unclear. The electron-phonon coupling strength was taken into account by the use of the superconducting tunneling data of McMillan and Rowell.[3] However, the electron-light matrix element was omitted.

There already exists in the literature a number of discussions of the Holstein mechanism. Pippard[4] has given an elegant qualitative description and Holstein[5] an elegant formalism for the normal-metal problem. Scher[6] has made numerical calculations based on Holstein's formalism in the local limit where the anomalous skin effect is ig-